

Polycrystalline $\text{ZnS}_x\text{Se}_{1-x}$ thin films deposited on ITO glass by MBE*

SHEN Da-ke(沈大可)^{1,2}, SOU I. K.², HAN Gao-rong(韩高荣)¹,
DU Pi-yi(杜丕一)¹, QUE Duan-lin(阙端麟)¹

(¹ State Key Laboratory of Silicon Material Science, Zhejiang University, Hangzhou 310027, China)

(² Department of Physics, Hong Kong University of Science and Technology, Hong Kong, China)

Received Mar. 1, 2002; revision accepted Apr. 15, 2002

Abstract: MBE growth of $\text{ZnS}_x\text{Se}_{1-x}$ thin films on ITO coated glass substrates were carried out using ZnS and Se sources with the substrate temperature ranging from 270 °C to 330 °C. The XRD $\theta/2\theta$ spectra resulted from these films indicated that the as-grown polycrystalline $\text{ZnS}_x\text{Se}_{1-x}$ thin films had a preferred orientation along the (111) planes. The evaluated crystal sizes as deduced from the FWHM of the XRD layer peaks showed strong growth temperature dependence, with the optimized temperature being about 290 °C. Both AFM and TEM measurements of these thin films also indicated a similar growth temperature dependence. High quality $\text{ZnS}_x\text{Se}_{1-x}$ thin film grown at the optimized temperature had the smoothest surface with lowest RMS value of 1.2 nm and TEM cross-sectional micrograph showing a well defined columnar structure.

Key words: MBE (molecular beam epitaxy), Polycrystalline $\text{ZnS}_x\text{Se}_{1-x}$ thin film, ITO glass, Structural characterizations

Document code: A

CLC number: TN304

INTRODUCTION

The growing interest in ultraviolet (UV) imaging technology can be due to its various possible applications in the fields of UV astronomy, environmental, biological science and medical instrumentation. It is well known that ZnS-based II-VI wide bandgap semiconductors enjoy the advantages of being highly resistive and UV light sensitive and having low dark noise, and are potentially good candidates as visible-blind UV imaging materials. Therefore, many studies had been carried out on the structural characterizations, electrical and opto-electronic properties of $\text{ZnS}_x\text{Se}_{1-x}$ thin films. Device-quality $\text{ZnS}_x\text{Se}_{1-x}$ thin films had also been obtained to make novel II-VI blue-green lasers (Ivanov et al., 1998) and visible-blind ultraviolet detectors (Sou et al., 1999). However, among most of the reported works on $\text{ZnS}_x\text{Se}_{1-x}$ thin films, only a few are about films of polycrystalline phase. These include the growth by the chemical solution growth technique on GaAs (110) substrates by Chaudhari et al. (1992), by the two-zone

hot wall evaporation technique on cleaned glass substrates by Gupta et al. (1992) and by atomic layer epitaxy technique on soda lime substrates by Ihanus et al. (1997). To the best of our knowledge, there is no report so far on studies of $\text{ZnS}_x\text{Se}_{1-x}$ alloy thin films grown on indium tin oxide (ITO) coated glass substrate by the molecular beam epitaxy (MBE) technique. In this paper, we will present the results of our studies on the MBE growth and various structural characterizations of $\text{ZnS}_x\text{Se}_{1-x}$ alloy thin films on ITO coated glass substrate for UV opto-electronic device applications.

EXPERIMENTS

All the $\text{ZnS}_x\text{Se}_{1-x}$ thin films used in this study were fabricated using a VG V80H MBE system. The pre-growth treatment of ITO coated glass is essential for achieving high quality $\text{ZnS}_x\text{Se}_{1-x}$ thin films. Commercial ITO glass substrates were first cleaned using Decon 90 detergent and then rinsed in de-ionized water

* Project supported by the National Science Council of PRC (No. 59910161981) and RGC grant from the Hong Kong Government under Grant (No. NS-FC/HKUST 35)

(18.2 M Ω cm) in an ultrasonic bath for 30 minutes at 40°C. After being baked dry at 100°C for 1 hour, they were loaded into the MBE system. Prior to the deposition, the substrates were preheated at 380°C for 20 minutes.

The growths of ZnS_xSe_{1-x} thin films were carried out using a ZnS compound source and an Se elemental source. Five samples were used in this study. Their substrate temperature was 270°C to 330°C (Table 1). Reflection high-energy electron diffraction (RHEED) was used to monitor the crystalline properties of the preheat treatment as well as the ZnS_xSe_{1-x} thin film growth. The as-grown thin films were cut into several pieces for various structural characterizations. Their structural perfection was examined by a Philips PW1830 powder x-ray diffraction system using Cu K α radiation ($\lambda = 1.540562$ Å). Standard $\theta/2\theta$ scans were performed with 2θ ranging from 15° to 55°. The chemical com-

positions of the films were determined using a Physical Electronics Phi5600 X-ray photoelectron spectroscopy (XPS) system. All the as-grown films were sputtered for 4 minutes prior to the XPS measurement to remove the surface contamination. The core levels Se 3d and S 2p were selected for quantitative analysis. The surface morphology of the as-grown ZnS_xSe_{1-x} thin films was studied in air using a Nanoscope IIIa atomic force microscope (AFM) from Digital Instruments. The scan range used was $3 \times 3 \mu\text{m}^2$. To investigate the microstructure of these films, high quality cross-sectional specimens with minimum damage for transmission electron microscopy (TEM) study were prepared first by mechanical polishing and then argon ion milling with successively decreasing ion-accelerating voltage. The cross-sectional images were then taken with a Philips CM20 TEM at 200 kV.

Table 1 Growth temperature and structural characterization results of five ZnS_xSe_{1-x} thin films

Sample	Substrate temperature(°C)	Se Composition (%)	Lattice constant (Å)	FWHM of XRD peak (deg.)	Crystal size (nm)	RMS roughness (nm)
Sample 1	330	35	5.486	0.752	12.1	7.7
Sample 2	310	51	5.544	0.679	13.4	5.7
Sample 3	290	21	5.467	0.474	19.2	1.2
Sample 4	280	42	5.515	0.623	14.6	4.7
Sample 5	270	28	5.477	0.674	13.5	8.8

RESULTS AND DISCUSSIONS

ITO films have high light transmittance, good electrical conductivity, excellent substrate adherence, hardness and chemical inertness. The extremely high quality large area substrates available at low cost make them particularly attractive substrate material. So they have been studied and are widely used in the semiconductor industry. In this work, two different types of crystal structural ITO coated glass were selected as the substrates. Let us define them as substrate A and B, respectively. XRD characterization performed on these bare substrates after wet chemical treatment revealed that they had very different crystalline characteristics. In Fig.1 a

and b are the $\theta/2\theta$ spectra obtained for substrate A and B, respectively. We also did post-growth XRD measurements of the unexposed part of the substrates (the sample holder contained a tantalum ring for sample mounting which covered part of the underlying substrate) used for the growth of samples 1 to 5, which yielded identical $\theta/2\theta$ spectra similar to those displayed in Fig.1. This indicated that the preheat treatment and the MBE growth did not cause any detectable modification of the ITO thin films. From inspection of Fig. 1a, one can see that the XRD spectra of substrate A shows the typical ITO fingerprints with the diffraction line from (222) planes being the dominant component. On the other hand, Fig. 1b indicates that the dominant component for substrate B is (400) which also shows a small shift of 0.2° towards a lower 2θ angle as com-

pared to the (400) peak of substrate A. The structural difference between these two types of ITO substrate was due to different manufacturing procedures. A difference in chemical composition might also be the cause since the results of XPS study on these two substrates indicated that the In/Sn ratio of substrate B was 2.7 times higher than that of substrate A.

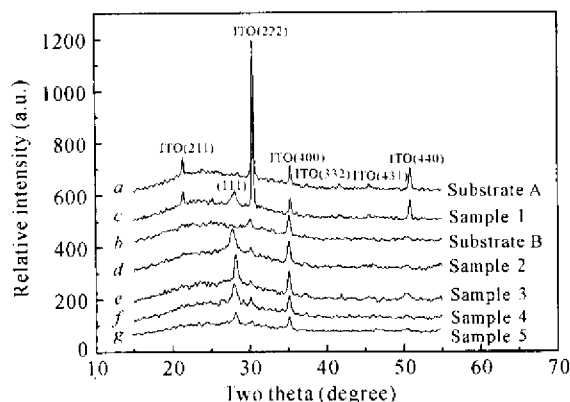


Fig.1 XRD spectra of two ITO substrates and five $\text{ZnS}_x\text{Se}_{1-x}$ /ITO thin films

In-situ RHEED studies showed that an amorphous pattern was usually obtained on the ITO surface prior to preheat treatment. At the end of the preheat treatment at 380°C , an expected pattern with several rings indicating polycrystalline materials was observed. The growth of $\text{ZnS}_x\text{Se}_{1-x}$ thin films led to a gradual change of the pattern to a different polycrystalline ring pattern. The postgrowth XRD spectra of samples 1 to 5 are displayed in Fig. 1c to 1g, respectively. These curves indicate that despite the large difference in crystalline orientation of the ITO thin films of substrate A and B, all the five as-grown $\text{ZnS}_x\text{Se}_{1-x}$ thin films show a single diffraction peak located near the standard (111) peak of cubic ZnS at $2\theta = 28.5^\circ$. The observed angular difference of XRD peaks among the five samples is believed to be due to the difference of Se composition in these films. Quantitative XPS analysis based on the ratio of the integrated peak area of Se 3d and S 2p (S $2p_{1/2}$ and S $2p_{3/2}$) core levels of these thin films revealed their Se compositions as listed in Table 1. The fluctuation of Se composition is believed to be due to the different sticking coefficient of Se and S atoms with the substrate temperature and the sticking coefficient

of S atoms being more sensitive to growth temperature than that of the Se atoms. The lattice constants evaluated from the XRD layer peaks are also shown in Table 1. The plot (Fig. 2) of the listed lattice constants versus the Se compositions shows linear relation, with the end points of the fitting straight line quite closely matching the standard lattice constants of ZnS and ZnSe, thereby verifying the existence of the $\text{ZnS}_x\text{Se}_{1-x}$ solid solution in our films. It is well known that pure ZnS and ZnSe exist in two crystalline phases, i. e., a cubic form with sphalerite structure and a hexagonal form with wurtzite structure. As to ZnS, the cubic form (c-ZnS) is the low temperature phase and the hexagonal form (h-ZnS) is the polymorph stable phase at high temperature. Because there are usually just a few peaks in the diffractograms, and many d-values between the two phases are overlapped or only have very small difference, it is difficult to distinguish these two phases from thin film samples (Ihanus et al., 1997). However, the lack of diffraction from any hexagonal planes indicated that the $\text{ZnS}_x\text{Se}_{1-x}$ thin films were polycrystalline, with zinc sulfide cubic structure, and showed (111) preferred orientation. Except for the rings and dots from ITO films, the TEM diffraction patterns of the five films were not containing any diffraction spot or ring of the hexagonal symmetry and the (111) ring of cubic symmetry being always the dominated component, agreed closely with the XRD observation results described above. Typical TEM diffraction pattern of sample 3 is inserted in Fig. 5.

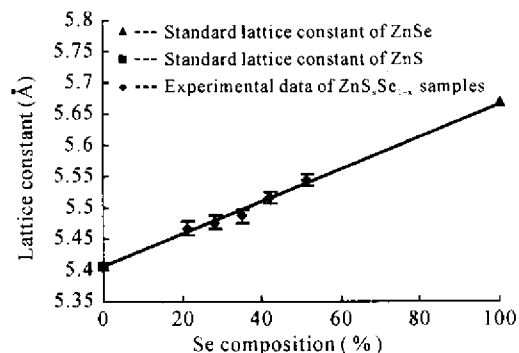


Fig.2 Lattice constants of the $\text{ZnS}_x\text{Se}_{1-x}$ thin films as a function of Se composition

The average crystalline sizes along the normal direction of the (111) planes of the $\text{ZnS}_x\text{Se}_{1-x}$ thin films were calculated from their full-width at half-maximum (FWHM) values of the XRD layer peaks by means of the Scherrer formula. The results are also listed in Table 1. The obtained crystalline sizes of the five samples seemed to indicate that there was an optimized substrate temperature at around 290°C at which the largest crystal size of 19.2 nm was obtained. A similar substrate temperature dependence was also observed in low-pressure metalorganic chemical vapor deposition (MOCVD) growth of polycrystalline ZnS thin films on ITO glass substrates as reported by Li et al. (1994) in which the optimized substrate temperature was around 225°C . Our AFM studies on the five $\text{ZnS}_x\text{Se}_{1-x}$ thin films indicated that their surface topological

features were similar but had different hillock dimensions. Their regional root-mean-square (RMS) values representing the degree of surface roughness were evaluated as listed in Table 1 showing that sample 3 which was grown at 290°C , had the smallest RMS value of 1.2 nm among the five samples. Fig. 3 shows the three-dimensional (3D) AFM images of the surface morphology of sample 1, 3 and 5 whose RMS roughness was 7.7 nm, 1.2 nm, and 8.8 nm, respectively. Figure 4 displays both the crystal sizes deduced from the FWHM values of the XRD layer peaks and the RMS values of roughness as a function of the substrate growth temperature. These two curves both clearly indicate that the optimized growth temperature for crystalline perfection and surface smoothness is around 290°C .

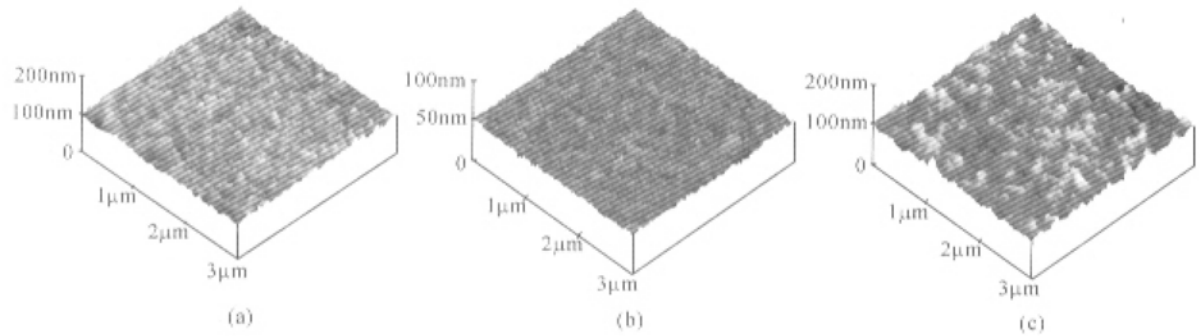


Fig.3 AFM surface image of sample 1, 3 and 5
(a) sample 1 at 330°C ; (b) sample 3 at 290°C ; (c) sample 5 at 270°C

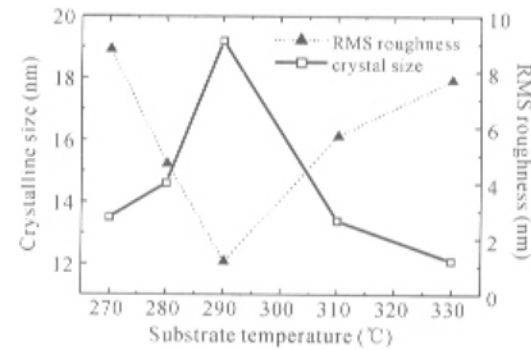


Fig.4 Crystalline sizes and RMS roughness of the $\text{ZnS}_x\text{Se}_{1-x}$ thin films as a function of growth temperature

Further evidence of this temperature dependence comes from the results of study of the thin films microstructure using cross-sectional TEM

imaging. The cross-sectional TEM images revealed that sample 3 grown at 290°C , as expected, had the best crystalline perfection among the five samples. Figure 5 shows its cross-sectional micrograph from which one can clearly see a well defined columnar structure grew above 250 nm from the substrate with lateral crystal dimension in the order of 500 – 700 angstroms. Fig. 6 shows the XPS depth profile of concentration of Zn, S, Se, In and O from the sample 3 deposited on ITO glass substrate. The Zn, S and Se XPS yields were almost constant within the thin film and with the interface between $\text{ZnS}_x\text{Se}_{1-x}$ thin film and ITO glass easily observed. This suggests that the film was compositionally homogeneous along the growth direction; that the interdiffusion between $\text{ZnS}_x\text{Se}_{1-x}$ and ITO was not serious in this deposition process; and that a

sharp interface had developed. The low Zn, S and Se XPS data yield at the surface was due to the surface contamination by oxygen element.

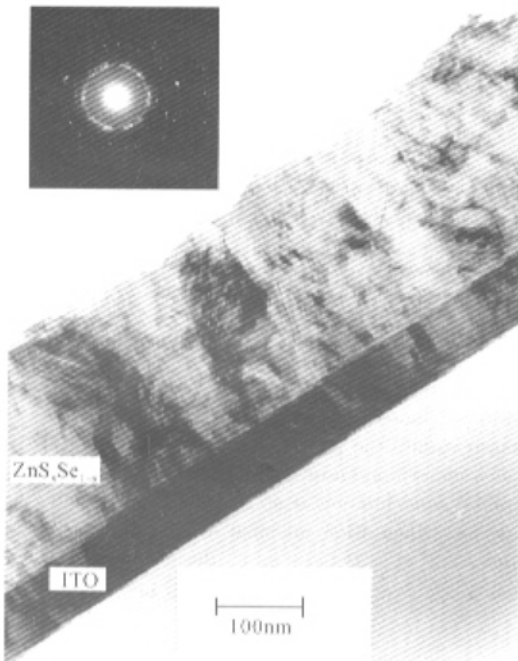


Fig.5 TEM cross-sectional image of a sample grown at 290°C. The inset is its TEM diffraction pattern

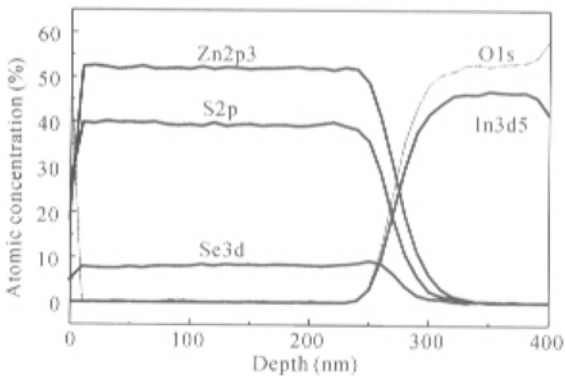


Fig.6 XPS depth profile of sample 3

CONCLUSIONS

This work researched the molecular beam epitaxial growth of ZnS_xSe_{1-x} thin films on ITO coated glass substrates using ZnS and Se effusion sources. The structural perfection of the as-grown thin films was characterized by various

techniques. The XRD spectra resulted from these films indicated that the as-grown polycrystalline ZnS_xSe_{1-x} thin films had a preferred orientation along the (111) planes. The evaluated crystal sizes as deduced from the FWHM of the XRD peaks were found to show strong growth temperature dependence with the optimized temperature at about 290°C. Atomic force microscopy (AFM) and transmission electron microscopy (TEM) measurements of these thin films also indicated a similar growth temperature dependence. The TEM cross-sectional micrograph of the sample grown at the optimized temperature showed a well defined columnar structure with lateral crystal dimension in the order of a few hundred angstroms. These features of the polycrystalline ZnS_xSe_{1-x} film with (111) plane preferred orientation, very smooth surface and reduced defect densities makes it attractive material for UV opto-electronic device applications.

References

- Chaudhari, G. N., Sardesai, S. N., Sathaye, S. D. and Rao, V. J., 1992. Structural properties of ZnS_xSe_{1-x} thin films on GaAs (110) substrate. *J. Materials Science*, **27**:4647-4650.
- Gupta, P., Bhattacharyya, D., Chaudhuri, S. and Pal, A. K., 1992. Preparation and characterization of polycrystalline ZnS_xSe_{1-x} films prepared by a two-zone hot wall technique. *Thin Solid Films*, **221**:154-159.
- Ihanus, J., Ritala, M., Leskelä, M. and Rauhalu, E., 1997. ALE growth of $ZnS_{1-x}Se_x$ thin films by substituting surface sulfur with elemental selenium. *Applied Surface Science*, **112**:154-158.
- Ivanov, S., Toropov, A., Sorokin, S., Shubina, T., Lebedev, A., Kop' er, P., Alferov, Z., Luganer, H. J., Reuscher, G., Keim, M., Fischer, F., Waag, A. and Landwehr, G., 1998. ZnSe-based blue-green lasers with a short-period superlattice waveguide. *Appl. Phys. Lett.*, **73**(15):2104-2106.
- Li, J. M., Chiang, J. D., Su, Y. K. and Yokoyama, M., 1994. The preparation of ZnS thin films on an indium tin oxide/glass substrate by low-pressure metalorganic chemical vapor deposition. *J. Cryst. Growth*, **137**:421-426.
- Sou, I. K., Ma, Z. H. and Wong, G. K. L., 1999. Photo-response studies of ZnSSe visible-blind ultraviolet detectors: A comparison to ZnSTe detectors. *Appl. Phys. Lett.*, **75**(23):3707-3709.